ELSEVIER

Journal of Alloys and Compounds 223 (1995) 81–86

Journal of ALLOYS AND COMPOUNDS

Thermally stimulated hydrogen desorption from zirconium and tantalum

D.E. Shleifman, D. Shaltiel, I.T. Steinberger *

The Racah Institute of Physics, The Hebrew University, Jerusalem 91904, Israel

Received 30 September 1994

Abstract

Thermal desorption experiments were performed in an ultrahigh vacuum chamber, employing a mass spectrometer equipped with mass multiplexing software. In some cases the sample was exposed to oxygen after hydrogenation. The temperature programmed desorption curves were analyzed using phenomenological theory for second-order H_2 desorption. The analysis showed the existence of up to three activation energies, associated with hydrogen desorption both from sites blocked by oxygen atoms and from others not affected by oxygen, combined with the activation energy due to the removal of oxygen. The oxygen reacts with hydrogen and leaves the sample in the form of water.

Keywords: Thermal stimulation; Hydrogen desorption; Zirconium; Tantalum

1. Introduction

The process of hydrogen desorption via the surface of a metal hydride depends on the surface composition. Unless extreme precautions are taken, the surface is contaminated by the presence of surrounding gases such as oxygen, CO_2 and others. These gases can react chemically with the metal and create an activation barrier for hydrogen desorption, much larger than the activation barrier of the clean metal surface.

The kinetics of hydrogen exchange between hydrogen interstitials and hydrogen in the gas phase is controlled by the reaction

$$H \text{ (in metal)} \longleftrightarrow \tfrac{1}{2}H_2 \text{ (gas)}$$

This kinetics can be studied by measuring the desorption rate of hydrogen from the metal into vacuum. Analysis of the desorption rate as a function of temperature and time reveals information on the activation energy barriers of the surface.

Pörschke et al. [1] investigated the desorption of hydrogen from tantalum foils, prepared by first introducing hydrogen into the foils and then exposing them to air. Two activation energies were derived from the hydrogen desorption rate at low and at high temperatures. The transition temperature T_t between the two regions was well defined within 10 degrees. The energies were associated with the barrier for the hydrogen to desorb from the contaminated surface and the barrier associated with diffusion of the contamination elements from the surface.

Exposing the surface to air introduces a large number of contaminating elements, thus it is not possible to determine the exact nature of the surface.

In this work the experiments were performed in an ultrahigh vacuum (UHV) system where it was possible to control the contaminating elements. In particular, for some experiments the surface was exposed to oxygen after the introduction of hydrogen. Two elemental metals were investigated, Ta and Zr. The most interesting result was that desorption of hydrogen also triggers the desorption of water, preceded by the reaction of oxygen with hydrogen to give H_2O. We report also on the various activation energies associated with the desorption of hydrogen.

2. Experimental procedure

The thermal desorption system comprised two chambers separated by a valve. The sample chamber had a volume of 0.44 l, it was connected to UHV pumps ensuring fast, constant speed pumping and was equipped with a VG SX200 quadrupole mass spectrometer. The

* Corresponding author.

SSDI 0925-8388(94)01497-3

preparatory chamber served for introduction of the gas, its volume was 0.063 l and the pressure in it could be monitored by an MKS Baratron capacitance manometer, to a resolution of 10^{-2} Pa. The volume ratio of the two chambers was known to an accuracy better than 1%. The samples were 6×7 mm^2 rectangles of thin foils of Ta or Zr, both 50 μm thick. Their purity was 99.9% for Zr and 99.95% for Ta. The sample could be heated conductively by tungsten wires and cooled by two 2.5 mm thick copper rods. These rods were part of a feedthru and could be cooled from the outside by liquid nitrogen; the tungsten wires were clamped to the copper rods. The sample temperature was measured by a chromel–alumel thermocouple, spot welded to the sample. The temperature of the sample was programmed by an appropriate PID (proportional integral differential loop tuning [2]) algorithm to vary linearly with time from 120 K to 1280 K. Special software was developed to enable recording of the temperature programmed desorption (TPD) curves of several masses concurrently. The molecular masses were normally chosen as follows: 2 (H_2), 4 (D_2), 16 (CH_4 or O), 18 (H_2O), 28 (CO or N_2) and 32 (O_2).

3. Sample preparation

Prior to mounting the sample it was cleaned using ethyl alcohol. Next the sample was mounted on its holder and washed (together with the holder) in an ultrasonic bath in a detergent solution, rinsed for several minutes in boiling deionized water and dried. After assembly, the chambers were connected, evacuated and baked until a base pressure of approximately 2×10^{-7} Pa was reached.

Pretreatment of the sample consisted of repeated hydrogen absorption–desorption cycles. H_2 was absorbed at temperatures between 650 K and 700 K for Ta, 600–650 K for Zr. Subsequently the sample was heated to about 970 K (Ta) or to 1070 K (Zr) to desorb the hydrogen still present in the sample, while pumping to a pressure of less than 10^{-6} Pa. This was followed by cooling the sample to 120 K and taking a hydrogen TPD curve. It was found that five absorption–desorption cycles decreased the maximum of the TPD curve by a factor of 100 or more, compared with the virgin sample. The maximum partial H_2 pressure recorded by the last TPD experiment was approximately 2×10^{-9} Pa. The pretreatment improved considerably the reproducibility of the results. We note that along with H_2 water was also desorbed from the sample (see below).

4. The experiments

TPD experiments were performed on samples prepared as described above, containing measured amounts of absorbed hydrogen. For some experiments, the sample was deliberately exposed to oxygen after hydrogen absorption. The procedure included in all cases the following steps, executed in the sample chamber with the valve to the preparatory chamber closed (except during treatment with H_2 or O_2). (1) The sample is precooled to 120 K. The main purpose of this step is to cool down, along with the sample, its immediate surroundings, so as to reduce later the H_2 background desorbed from the surroundings and enable very fast cooldown from high temperatures. (2) The sample is heated to 970 K (Ta) or 1070 K (Zr), while monitoring H_2. The heating was left on for 400 s; this was sufficient to desorb most of the hydrogen. (3) The sample is cooled to 120 K. The cooling was very fast (approximately 15 s) in order to minimize oxidation from the residual gas. (4) The pumping is stopped; the immediate rise in pressure is to about 10^{-4} Pa. (5) Hydrogen is added via the preparatory chamber and the sample is heated (up to 600 K for Ta, 300 to 500 K for Zr) to ensure hydrogen absorption. The amount of hydrogen absorbed by the sample is determined from the volumes of the two chambers and the measured pressure drop. (6) After the required amount of hydrogen has been absorbed, the sample is cooled quickly to 150 K to stop absorption. (7) The two chambers are pumped down to 2×10^{-7} Pa followed by closure of the valve between them. To obtain oxidized samples, the above operations were followed by heating the sample at 470 K in oxygen (at a pressure of the order of 100 Pa) for 50 min. The amount of oxygen absorbed was much too low for determination by the Baratron gage. At 470 K both Ta and Zr oxidize but do not desorb hydrogen. After oxidation the sample was cooled down again to 150 K and the chamber pumped down to UHV. Most TPD experiments started (with one exception, see below) at 120 K.

5. Results

The samples prepared as stated above underwent temperature programmed desorption experiments; the usual heating rate was 1 K s^{-1}. At first TPD curves were taken concurrently for all mass numbers listed above, up to temperatures of 1250 K. It was found that the gases desorbed comprised mainly hydrogen and water. No water was detected from samples that had not absorbed hydrogen. There was a very small peak (less than 2×10^{-10} Pa at maximum) for mass 32 and a substantially larger peak for mass 16. It follows that a very small amount of O_2 desorbed but appreciably

more CH_4. As a check of the role of the sample in the desorption process we substituted a thin (approximately 0.25 mm) copper foil for the sample; it underwent similar treatment as the Ta and Zr foils. The TPD experiment with this foil did not show peaks for any of the gases listed, but there was a slight, gradual increase in the H_2 and O_2 background with increasing temperature. We infer that the results described below do indeed pertain to Ta or Zr and not, for example, to the sample mountings.

Fig. 1 presents results on Ta, without deliberate oxidation. Fig. 1(a) shows TPD curves for H_2 and H_2O taken concurrently. It is clearly seen that the maxima of the two curves occur at the same temperature, namely at 785 K. The ratio r of the amounts of hydrogen and water molecules (obtained from the areas of the TPD curves and proper calibration) is 46; however the instantaneous ratio of the mass spectrometer signals is not constant. The two curves clearly indicate that (1) oxygen must have been present in the sample from the outset, in spite of the fact that we did not oxidize it deliberately, and (2) one of the desorption channels of hydrogen involves the formation of water in the sample or on its surface.

Fig. 1(b) shows results of analysis of the hydrogen curve of Fig. 1(a). The abscissa is proportional to the reciprocal temperature. The right-hand scale refers to the ratio x of the number of hydrogen atoms to that of tantalum atoms in the sample as calculated from the number of hydrogen atoms initially absorbed and the number of hydrogen molecules desorbed. The left-hand scale presents $\ln(-x^{-2}\,dx/dt)$. Plots of $\ln(-x^{-2}\,dx/dt)$ vs. the reciprocal temperature are very convenient representations of second-order desorption processes [3]. The slopes give activation energies directly (see also Section 6 below). It is seen that the slope changes only slightly in the graph in question. $E_{low} = 1.4$ eV at lower temperatures and $E_{high} = 1.2$ eV at higher temperatures.

Figs. 2(a) and (2b) correspond in every respect to Figs. 1(a) and 1(b), but they refer to the Ta foil that underwent deliberate oxidation after hydrogen had been adsorbed. At first glance, Fig. 2(a) resembles Fig. 1(a), but the ratio r is now only 25, obviously because of the higher oxygen content. Dramatic differences are evident, however, if one compares the $\ln(-x^{-2}\,dx/dt)$

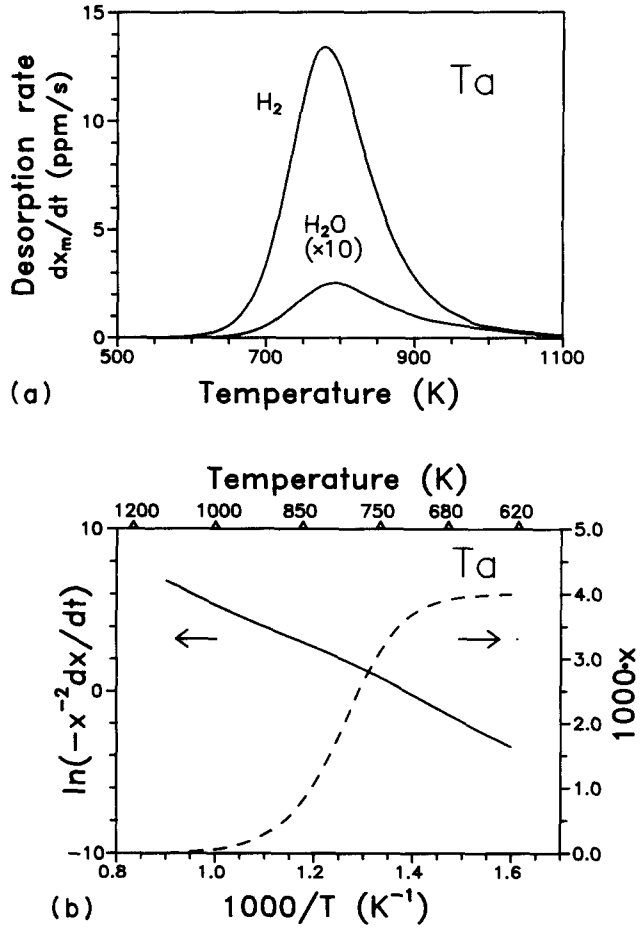

Fig. 1. (a) TPD of H_2 and H_2O from $TaH_{0.0040}$. x_m is the number of molecules desorbed, divided by the number of Ta atoms in the sample. (b) Obtained from Fig. 1(a), hydrogen data. x is equal to the atomic ratio in the bulk, $x \equiv x_0 - 2x_m$; x_0 is the initial atomic ratio: – – –, x vs. 1000/T; ——, $\ln(-x^{-2}\,dx/dt)$ vs. 1000/T.

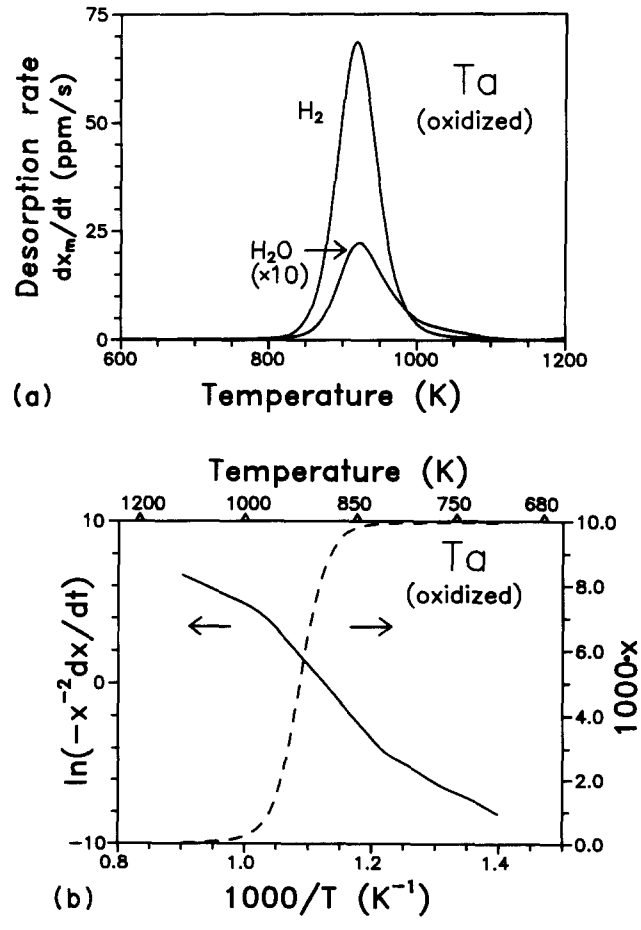

Fig. 2. As Fig. 1, for $TaH_{0.010}$ (deliberately oxidized sample).

plot in Fig. 2(b) with that in Fig. 1(b): in Fig. 2(b) three very distinct slopes are observed, corresponding to activation energies $E_{low} = 2.0$, $E_{med} = 3.8$ and $E_{high} = 1.7$ eV (E_{med} refers to medium temperatures) in contrast with the two slopes of Fig. 1(b).

Figs. 3(a) and 3(b) are constructed as the previous corresponding figures.They present results obtained for a Zr foil, not deliberately oxidized. Again in Fig. 3(a) the hydrogen TPD peak coincides with the peak for water; the ratio r is 22. The dependence of $\ln(-x^{-2}\,dx/dt)$ on $1000/T$ is again roughly linear; the activation energies are $E_{low} = 1.4$, $E_{high} = 0.9$ eV.

Figs. 4(a) and 4(b) refer to the Zr foil of Figs. 3(a) and 3(b), but after deliberate oxidation. The hydrogen and the water TPD peaks in Fig. 4(a) again coincide to a good approximation; the ratio r is 18. The $\ln(-x^{-2}\,dx/dt)$ vs. $1000/T$ plots now have three distinct slopes, namely $E_{low} = 0.9$, $E_{med} = 3.4$, $E_{high} = 0.6$ eV. The change with respect to Fig. 3(b) is very prominent, as is the case if Fig. 2(b) is compared with Fig. 1(b).

Fig. 5 illustrates the dependence of the TPD curves on the initial dose of hydrogen, for the Zr foil without deliberate oxidation. The areas increase proportionally (within the margin of error) with the hydrogen dose. Moreover, both the low temperature onsets and the

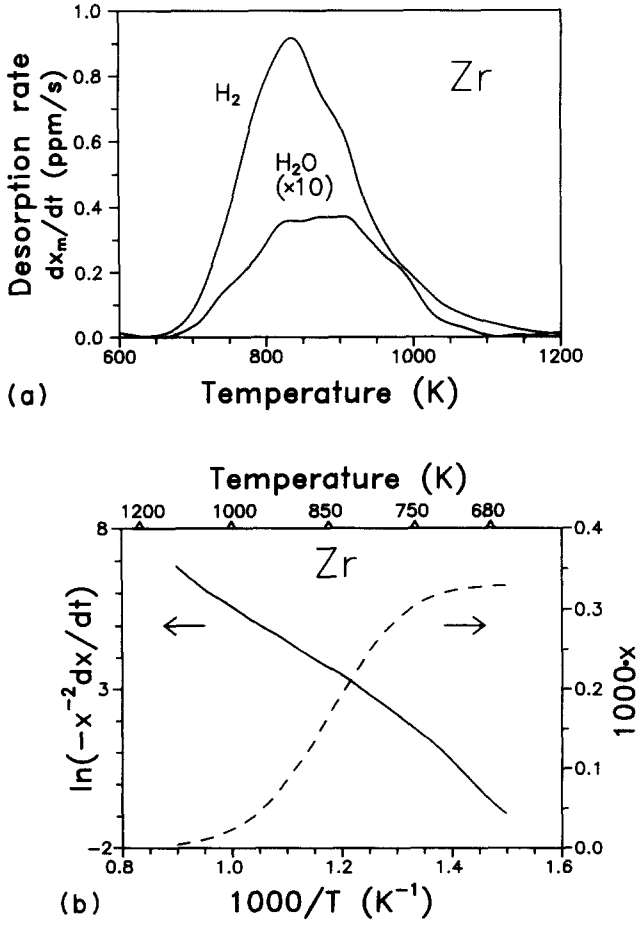

Fig. 3. As Fig. 1, for $ZrH_{0.00033}$.

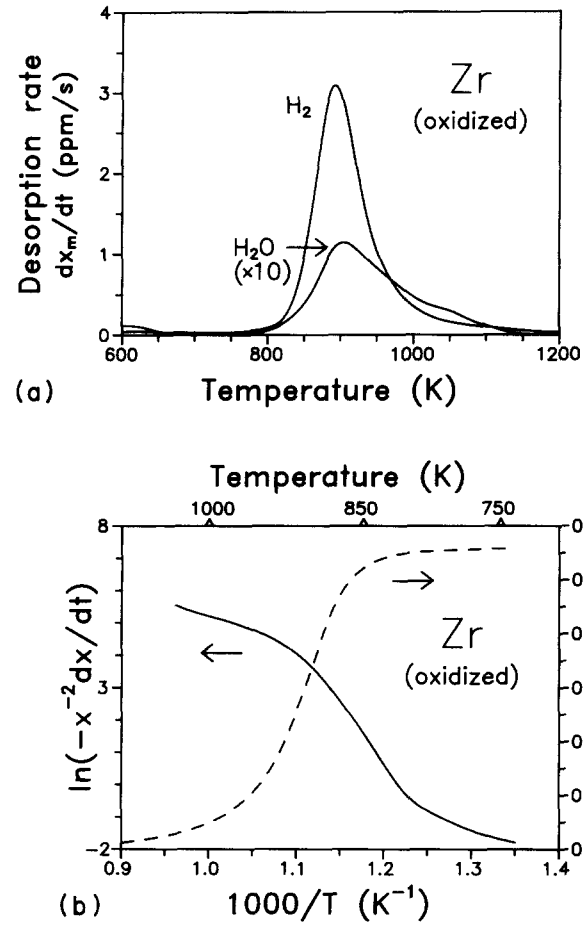

Fig. 4. As Fig. 1, for $ZrH_{0.00057}$ (deliberately oxidized sample).

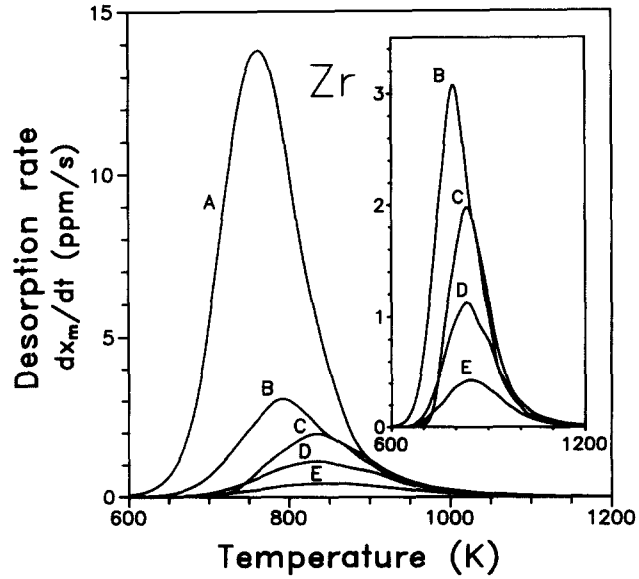

Fig. 5. Family of TPD curves for (A) $ZrH_{0.0035}$, (B) $ZrH_{0.0011}$, (C) $ZrH_{0.00060}$, (D) $ZrH_{0.00033}$, (E) $ZrH_{0.00013}$. The experiments started after fast cooling to 120 K, except C, see text.

positions of the maxima shift to lower temperatures with increasing hydrogen dose. This behavior strongly supports the assumption of second-order desorption kinetics. Curve C differs from the rest. In this case the sample was cooled to 300 K in about the same time (approximately 15 s) as was usually used for cooling to 120 K. The onset and the maximum are shifted to higher temperatures. Such shifts can be caused by oxidation, as can be seen by comparing Fig. 3(b) with Fig. 4(b). We infer that under the conditions of curve C the sample was appreciably oxidized from the ambient residual gas.

6. Discussion

The effect of a second gas, usually oxygen, on hydrogen desorption from Ta and Zr hydrides has been studied repeatedly in the past [4,5]. The present work focuses on the α-phase of the hydrides; it was performed in a UHV chamber with a base pressure of 2×10^{-7} Pa and utilizes mass multiplexing for TPD. The amount of H_2 absorbed was monitored carefully during the preparation of the samples, but monitoring the absorbed oxygen was impossible because of the small amounts of oxygen involved. The amount of oxygen desorbed could be estimated from the area ratios of the TPD curves for hydrogen and for water; the former could be calibrated in absolute terms during the absorption process (see above). Table 1 summarizes the amount of oxygen desorbed from the four samples to which Figs. 1–4 refer. It also includes an estimate for the number of oxygen planes that one would obtain if all oxygen atoms were arranged in planes of the same atomic density as the metal.

When looking at Table 1 it becomes immediately evident that the amount of water desorbed along with hydrogen is affected by deliberate exposure to oxygen but the change in the hydrogen-to-water ratio does not exceed the factor 2. Obviously the samples contained oxygen even without deliberate exposure; the oxygen might have been present in the metal from the outset or absorbed as an impurity of the hydrogen. Even so, the deliberate exposure to oxygen has a dramatic effect on the reaction kinetics, as is evident from comparison of Fig. 2(b) and Fig. 1(b) and of Fig. 4(b) and Fig. 3(b). If oxygen is added, the activation energy for hydrogen desorption in the middle temperature range (i.e. around the maximum of the peak) increases dramatically.

The interpretation of these results is facilitated by the fact that the removal of oxygen from the sample was monitored by the TPD curve of water, concurrently with TPD of hydrogen. The analysis is based on the assumption that the rate-limiting step for hydrogen desorption is on the surface. Accordingly, we assume that the diffusion of hydrogen in the bulk to the surface is much faster than its desorption from the surface. We assume further that the desorption is a second-order process. It follows that if x is the atomic concentration of hydrogen then

$$-\frac{dx}{dt} = M_s \nu x^2 \exp(-2\Delta E/kT) \quad (1)$$

where M_s is proportional to the concentration of active sites on the surface, ν is the jump frequency, ΔE is the activation energy for the desorption reaction per hydrogen atom, t is the time and T is the absolute temperature. With such kinetics the plot of $\ln(-x^{-2}\, dx/dt)$ vs. $1/T$ should be a straight line with slope $-2\Delta E/k$, as is indeed observed for samples that had not been deliberately exposed to oxygen. The conclusions drawn from Fig. 5 also support strongly the second-order kinetic model.

The qualitative explanation of the observations (Figs. 1(b), 2(b), 3(b) and 4(b)) is as follows. We assume that the metal surface presents two different activation energies for hydrogen desorption, $\Delta E_O > \Delta E_f$. The difference between the two energies is due to the well known blocking action of oxygen for the desorption of hydrogen from hydrides [6]: ΔE_O is the activation energy corresponding to a site of type I, affected by the vicinity of an oxygen atom (or ion), and ΔE_f refers to sites free of oxygen (of type II). We assume furthermore that a site of type I can become a site of type II by the desorption of oxygen (in the form of water). At the lowest temperatures only sites of type I are available, since the oxygen atoms block all possible desorption paths, $E_{low} = 2\Delta E_O$. With increasing temperature more and more oxygen atoms desorb, turning sites of type

Table 1
Activation energies E_{low}, E_{med}, E_{high}, activation energy E_d for transforming sites of type I to sites of type II (see text), number of hydrogen and water molecules desorbed, their ratio r and the number of equivalent layers (see text) for different samples

Chemical formula	E_{low} (eV)	E_{med} (eV)	E_{high} (eV)	E_d (eV)	H_2 desorbed	H_2O desorbed	r	Equivalent layers
$TaH_{0.0040}$	1.43 ± 0.05		1.20 ± 0.06		2.15×10^{17}	4.66×10^{15}	46.2	8.0
$TaH_{0.010}$	1.95 ± 0.13	3.79 ± 0.04	1.69 ± 0.14	2.10 ± 0.15	5.51×10^{17}	2.17×10^{16}	25.4	37.0
$ZrH_{0.00033}$	1.41 ± 0.08		0.90 ± 0.05		1.63×10^{16}	7.43×10^{14}	21.9	1.3
$ZrH_{0.00057}$	0.92 ± 0.11	3.40 ± 0.05	0.64 ± 0.11	2.76 ± 0.12	2.85×10^{16}	1.57×10^{15}	18.2	2.7

I to sites of type II. When the oxygen desorption is completed, the remaining hydrogen atoms see only sites of type II, with a lower activation energy $E_{high} = 2\Delta E_f$. In fact, the lowest-temperature parts of the $\ln(-x^{-2}\,dx/dt)$ vs. $1/T$ curves reveal a consistently higher activation energy than the highest-temperature parts, in full accord with the above picture, in all graphs.

The steep central sections of Figs. 2(b) and 4(b), and the absence of such sections in Figs. 1(b) and 3(b) leads us to the tentative assumption that by deliberate oxidation we create somewhat different kinds of oxygen centers than those that were already present in the sample. The difference would be manifest in the activation energy E_d of their desorption: for the "native" oxygen defects (Figs. 1 and 3) $E_d = 0$, while for those created by deliberate oxidation (Figs. 2 and 4) $E_d > 0$. It follows that for Figs. 1 and 3 the removal of oxygen along with hydrogen should be gradual, starting at the lowest temperatures, while for Figs. 2 and 4 oxygen can be removed only at higher temperatures, with the activation energy $E_{med} = E_d + 2\Delta E_f$ obtained from the central steep rise of the plots [1]. From these considerations we obtain $E_d = 2.1$ eV for Ta and $E_d = 2.8$ eV for Zr. Further detailed experiments are needed to test the above assumption.

For hydrogenated Ta samples that had been exposed to air, Pörschke et al. [1] recorded TPD curves similar to our Fig. 2(b), but without the highest-temperature part. They attributed the steep part of the $\ln(-x^{-2}\,dx/dt)$ vs. $1000/T$ curves to dissolution of the segregated oxide surface layer by diffusion into the bulk. However, their experimental results are in full accord with our interpretation, supported by simultaneous hydrogen and water TPD experiments.

A detailed quantitative formulation of this model will be published elsewhere.

Acknowledgement

The authors wish to thank the Deutsche Forschungsgemeinschaft (DFG) for a grant financing the project.

References

[1] E. Pörschke, D. Shaltiel, K.H. Klatt and H. Wenzl, *J. Phys. Chem. Solids, 47* (1986) 1003.
[2] J. Ziegler and N. Nichols, *Trans. ASME, 64* (1942) 759.
[3] B. Gumhalter, M. Milun and K. Wandelt, *Selected Studies of Adsorption on Metal and Semiconductor Surfaces,* Forschungszentrum Jülich, Jülich, 1990.
[4] R.G. Spulak, Jr., *J. Less-Common Met., 153* (1989) L25.
[5] D.A. Asbury, G.B. Hoflund, W.J. Peterson, R.E. Gilbert and R.A. Outlaw, *Surf. Sci., 185* (1987) 213.
[6] L. Schlapbach, A. Seiler, F. Stucki and H.C. Siegmann, *J. Less-Common Met., 73* (1980) 145.